☙

Large-scale simulation of the spin-lattice dynamics in ferromagnetic iron

Pui-Wai Ma and C. H. Woo[*]

Department of Electronic and Information Engineering, The Hong Kong Polytechnic University, Hong Kong SAR, China

S. L. Dudarev

EURATOM/UKAEA Fusion Association, Culham Science Centre, Oxfordshire OX14 3DB, United Kingdom
and Department of Physics, Imperial College, Exhibition Road, London SW7 2AZ, United Kingdom

We develop a dynamical simulation model for magnetic iron where atoms are treated as classical particles with intrinsic spins. The atoms interact via scalar many-body forces as well as via spin orientation dependent forces of the Heisenberg form. The coupling between the lattice and spin degrees of freedom is described by a coordinate-dependent exchange function where the spin orientation dependent forces are proportional to the gradient of this function. The spin-lattice dynamics simulation approach extends the existing magnetic potential treatment to the case where the energy of interaction between the atoms depends on the relative noncollinear orientations of spins. An algorithm for integrating the linked spin-coordinate equations of motion is based on the second-order Suzuki-Trotter decomposition for noncommuting operators of evolution for coordinate and spin variables. The notions of the spin thermostat and the spin temperature are introduced through the combined application of the Langevin spin dynamics and the fluctuation-dissipation theorem. We investigate several applications of the method, performing microcanonical ensemble simulations of adiabatic spin-lattice relaxation of periodic arrays of 180° domain walls, and isothermal-isobaric ensemble dynamical simulations of thermally equilibrated homogeneous systems at various temperatures. The predicted isothermal magnetization curve agrees well with the experimental data for a broad range of temperatures. The equilibrium as well as time-correlation functions of spin orientations exhibit the presence of short-range magnetic order above the Curie temperature. Furthermore, short-range order spin fluctuations are shown to contribute to the thermal expansion of the material. Our analysis illustrates the significant part played by the spin degrees of freedom in the dynamics of motion of atoms in magnetic iron and iron-based alloys. It also shows that the spin-lattice dynamics algorithm developed in this paper offers a viable way of performing large-scale dynamical atomistic simulations of magnetic materials.

I. INTRODUCTION

The study of dynamics of magnetic degrees of freedom is a rapidly developing area of research in the field of advanced materials and technologies. Understanding microscopic processes involving the dissipation of energy and angular momentum in spin currents has direct technological implications for spintronics.[1–3] The propagation and redistribution of energy and angular momentum in the spin subsystem,[4,5] as well as between the lattice and the spin subsystems[6–9] are also actively investigated. There is consensus that a viable atomistic simulation of a magnetic material at a finite temperature requires treating the dynamics of both the spin and the lattice degrees of freedom.

A. Coupled spin-lattice dynamics

In a transition metal, the intrinsic angular moments (spins) of atoms—and the associated magnetic moments—are formed primarily due to the intraatomic exchange interaction between d electrons in the partially filled atomic d shells. The interplay between the intraatomic exchange and interatomic quantum hopping of electrons gives rise to ferromagnetic, antiferromagnetic, or complex noncollinear ordering of magnetic moments. In a tight-binding treatment, e.g., the Hubbard model,[10] the concept of a localized "atomic

spin" is justified for the itinerant magnets. Due to the simultaneously localized and itinerant nature of the hybridized s and d electrons in a transition metal, the directions and magnitudes of the atomic spins are both variable quantities.[11] Interatomic spin-spin interaction of the Heisenberg form can also be introduced using the concept of an effective intersite exchange coupling function. Spin waves are excited by thermal agitation.[12–14] The adiabatic treatment of spin and lattice subsystems does not apply at high temperatures where interaction between phonons and magnons is non-negligible.[12]

Within the frameworks of density-functional theory (DFT) for noncollinear magnetic ground states in the adiabatic approximation, spin dynamics (SD) and spin configurations,[15,16] spin-wave spectra,[17,18] and the dynamical spin susceptibility[19] were investigated. Following an alternative approach, a dynamical treatment of magnetic moments that takes into account the stochastic effects was introduced by Kakehashi *et al.*[20–23] Self-consistency of coupling between the spin and the lattice subsystems is usually not fully accounted for.

The occurrence of magnetic anisotropy, magnetoelasticity, and magnetostriction provides evidence that the atomic spin orientations and the symmetry of the lattice are coupled. Spin waves and phonons were explicitly included in the thermodynamic treatment of the ferromagnetic free energy in the early work by Kittel and Abrahams.[24] Antropov *et al.*[25] com-

bined the *ab initio* SD with *ab initio* molecular dynamics (MD) to take into account the spin-lattice interactions. Although both the stochastic (based on the Fokker-Planck equation) and deterministic (based on the Nose-Hoover thermostat) methods were considered as possible ways of treating the finite temperature case, only the 0 K calculations for fcc Fe were actually performed.

In cases where energy and angular momentum exchange involving the spin and the lattice subsystems needs to be considered in the nonadiabatic context, the Landau-Lifshitz (LL) or the Gilbert equations[26] were applied to model dissipation and interaction with the thermal reservoir. The magnitude of the dimensionless damping constant characterizing the rate of dissipation can be estimated from the ferromagnetic resonance (FMR) absorption linewidth.[27–32] Theoretical argument suggests that the damping constant depends on the temperature,[28,29] composition,[30,31] and topological symmetry[31,32] of a particular system, and may even have a tensor form.[33] Strictly speaking, since the original LL and Gilbert equations are both purely dissipative, they cannot be used to describe the thermal equilibration of the spin subsystem, as the spin subsystem would always relax toward the ground-state configuration. If one defines the spin temperature T_s and assumes that the heat flow in and out of the spin subsystem is proportional to the difference ΔT between the temperatures of the spin subsystem and that of the reservoir,[9] the dissipation rate can be taken as being proportional to ΔT and can be positive or negative, driving the transfer of energy and angular momentum in and out of the spin subsystem. However, defining the spin temperature proves to be a more subtle problem because spin dynamics is described by first-order differential equations and the notion of kinetic energy cannot be introduced to define temperature as it is normally done in MD. Brown Jr.[34] proposed a stochastic method based on the fluctuation-dissipation theorem[35,36] (FDT) for a classical spin system. Using this, the spin temperature can be defined by matching the solution of the corresponding Fokker-Planck equation to the Gibbs distribution. For example, the FDT provides a way of defining the temperature of a Brownian particle interacting with the environment.[36] The stochastic spin dynamics equations were also investigated in Refs. 37 and 38.

Recently Kadau *et al.*[39] considered a classical Hamiltonian for the coupled spin and lattice degrees of freedom and investigated the phase stability of the model using a Monte Carlo approach. The Invar effect and the antiferromagnetic ordering of spins in a FeNi alloy were successfully reproduced, confirming the effect of spin degrees of freedom on the phase stability and on the elastic properties of the material.

B. Molecular dynamics for a magnetic material

At a fundamental level, the behavior of a magnetic material at finite temperature is determined both by its spin-dependent electronic structure and by the thermodynamics involved. *Ab initio* approaches to the treatment of electronic structure are only able to describe very small systems, which are hardly sufficient to address the statistical nature of the

atomic and electronic excitations at a finite temperature. Thus, simulating the dynamics of formation and migration of defects, dislocations, magnetic domains, grain boundaries, phase transformations and collision cascades initiated by incident energetic particles, requires treating systems containing a large number of atoms. A realistic simulation must also be able to describe various saddle-point configurations and the many-body excited states associated with those saddle points, not to speak of the energy dissipation and entropy production due to scattering of interacting phonons and magnons. There is yet no atomistic simulation method comparable with MD that would provide a mathematical framework suitable for this purpose.

Even in an MD simulation, magnetic interatomic potentials must include the interaction between neighboring spins, as discussed by Dudarev and Derlet[40,41] (DD) and by Ackland.[42] Nevertheless, the DD potential effectively treats magnetism as a 0 K phenomenon, assuming that the atomic spins are all aligned, and hence, the treatment of complex noncollinear spin configurations at a finite temperature remains outside its realm of applicability. As indicated in the foregoing, the real challenge to MD simulations is partially associated with the accuracy of the magnetic potential and this mainly comes from the need to explicitly include the directional spin degrees of freedom. These degrees of freedom describe interatomic forces associated with the thermal orientational disorder of magnetic moments and result from the interaction between spin waves (magnons) and lattice vibrations (phonons).

In this paper, we develop a reformulation of MD that includes the spin degrees of freedom on equal footing with the lattice degrees of freedom, treating the coupled spin and lattice excitations within a unified simulation framework and taking the position of atoms and orientation of atomic spins as independent variables. The equations of motion for spins are derived from a generalized Heisenberg Hamiltonian where the exchange coupling function is fitted to the *ab initio* data and where the scalar part of the interatomic interaction is given by the magnetic DD potential.[40,41,43] These equations form the basis for the spin-lattice dynamics (SLD) algorithm. The SLD equations are integrated using the second-order Suzuki-Trotter decomposition (STD) (Refs. 44–48) technique for the noncommuting operators of evolution for the lattice and spin degrees of freedom. The position of each atom and the orientation of atomic spin are determined at each simulation time step. The coordinate dependence of the exchange coupling function links evolving spin and lattice subsystems and is responsible for the spin-orientation-dependent part of interatomic forces. The "spin temperature" is introduced using the stochastic Langevin dynamics formulation[34] combined with the fluctuation-dissipation theorem. Several examples described below illustrate the fairly broad range of potential applications of the SLD simulation algorithm.

II. METHOD

A. Equations of motion

The total "potential" energy of a system of N magnetic atoms is a function of the positions $\{\mathbf{R}_k\}$ of atoms and

their vector magnetic moments $\{\mathbf{M}_k\}$. Since the quantum-mechanical Hamiltonian of the system is invariant with respect to the choice of the spin-quantization axis, the expectation value for energy must also be invariant with respect to the choice of this axis. A sufficiently general functional form satisfying this invariance principle is[49]

$$E(\{\mathbf{R}_k\},\{\mathbf{M}_k\}) = E^{(0)}(\{\mathbf{R}_k\}) + \sum_i E^{(1)}(\{\mathbf{R}_k\})\mathbf{M}_i^2$$

$$+ \sum_i E^{(2)}(\{\mathbf{R}_k\})(\mathbf{M}_i^2)^2$$

$$+ \sum_{i,j} E^{(3)}(\{\mathbf{R}_k\})\mathbf{M}_i \cdot \mathbf{M}_j + \cdots \quad (1)$$

The first three terms in this series can be grouped together and incorporated into a many-body potential term, which can be treated as a "scalar" part of energy, independent of the orientations of atomic spins. The last term is the lowest-order intersite exchange coupling term. By minimizing the energy with respect to the *magnitude* of magnetic moments, (eliminating in this way the *high-energy* part of the spectrum of electronic excitations) and by retaining only the lowest-order exchange coupling term, Eq. (1) can be written in as[49]

$$E(\{\mathbf{R}_k\},\{\mathbf{e}_k\}) = U(\{\mathbf{R}_k\}) - \frac{1}{2}\sum_{i,j} J_{ij}(\{\mathbf{R}_k\})\mathbf{e}_i \cdot \mathbf{e}_j, \quad (2)$$

where $\mathbf{e}_k$ are the unit vectors of atomic spin directions and the magnitude of magnetic moments is absorbed into the definition of the exchange function $J_{ij}(\{\mathbf{R}_k\})$. Although from Eq. (2) it may appear that only the spin direction represents a state variable, the magnitude of the magnetic moment also varies dynamically through the dependence of the moment on the local atomic environment $\{\mathbf{R}_k\}$ according to the magnetic term of the DD potential.[40,41] We also note that the longitudinal spin fluctuations in bcc Fe are relatively insignificant[50] and the magnitude of magnetic moments in the paramagnetic and ferromagnetic phases is not very different. However, the longitudinal fluctuations of magnetic moments play a significant part in metals such as Ni.[50,51]

The corresponding effective classical Hamiltonian can now be written as[44,45,52]

$$H = \sum_i \frac{\mathbf{p}_i^2}{2m_i} + U - \frac{1}{2}\sum_{i,j} J_{ij}\mathbf{e}_i \cdot \mathbf{e}_j. \quad (3)$$

This classical Hamiltonian treats the lattice and spin degrees of freedom as coupled subsystems. The third term describes the exchange coupling between directions of atomic spins, which can be treated as an effective coordinate and spin orientation dependent interatomic potential.[13] To facilitate the discussion, we call this term the spin-potential, as opposed to the usual many-body interatomic potential U describing the spin direction independent scalar interaction between the atoms. We note that the spin-dependent potential is a function of orientations of the spins and, in a general case, it is also a many-body function of atomic coordinates. Since a regular
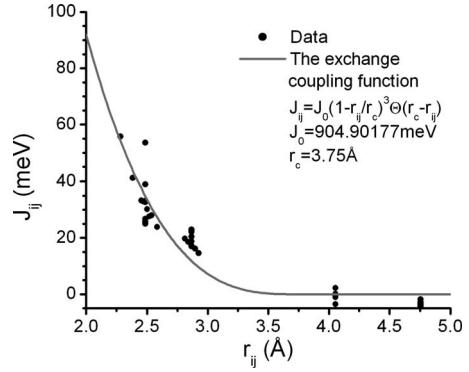
FIG. 1. Exchange function J_{ij} shown as a function of interatomic distance r_{ij} and is compared with data taken from Refs. [17] and [55]. The assumed form for the exchange function is $J_{ij}(r_{ij}) = J_0(1 - r_{ij}/r_c)^3 \Theta(r_c - r_{ij})$, where $J_0 = 904.90177$ meV and $r_c = 3.75$ Å.

method for deriving the scalar and the spin potentials from a many-body quantum Hamiltonian for interacting electrons is not yet available,[49] we adopt the following semiempirical classical approximation:

$$H = \sum_i \frac{\mathbf{p}_i^2}{2m_i} + H_{DD} + (H_{\text{spin}} - H_{\text{spin}}^{\text{ground}})$$

$$= \sum_i \frac{\mathbf{p}_i^2}{2m_i} + H_{DD} - \frac{1}{2}\sum_{i,j} J_{ij}(\mathbf{e}_i \cdot \mathbf{e}_j - 1), \quad (4)$$

where the first term is the kinetic energy of the atoms, H_{DD} is the DD magnetic potential,[40,41] $H_{\text{spin}} = (1/2)\Sigma_{i,j}J_{ij}\mathbf{e}_i \cdot \mathbf{e}_j$ is the spin Hamiltonian, and $H_{\text{spin}}^{\text{ground}}$ is the ground-state energy for the spin subsystem at 0 K. Using this notation, we write $U = H_{DD} + (1/2)\Sigma_{i,j}J_{ij}$. The functional form of Hamiltonian (4) ensures that the energy and the atomic forces are correctly defined in the collinear ferromagnetic state at 0 K.

In lattice models, the exchange function J_{ij} is given by a set of discrete values corresponding to a set of interatomic nearest-neighbor distances characterizing a particular lattice.[13,24] In our formulation, we take it as a continuous function of atomic coordinates.[52,53] Here we further assume that J_{ij} is a pairwise function of atomic coordinates and in effect treat J_{ij} as a mid-to–long range part of the Bethe-Slater curve.[54] Using *ab initio* calculations, Morán *et al.*[17] and Sabiryanov *et al.*[55] investigated how the exchange function varied as a function of interatomic distance. We parameterized J_{ij} by fitting a continuous function to the data points given in Table I of Ref. [17] and in Fig. 2 of Ref. [55]. Given the approximate nature of the fit and the approximate nature of the pairwise representation for the exchange function, we use only a single third-order polynomial to describe the radial dependence of J_{ij}, namely,

$$J_{ij}(r_{ij}) = J_0(1 - r_{ij}/r_c)^3 \Theta(r_c - r_{ij}), \quad (5)$$

where $r_{ij} = |\mathbf{R}_i - \mathbf{R}_j|$ and $\Theta(r_c - r_{ij})$ is the Heaviside step function. We chose the cut-off distance $r_c = 3.75$ Å in the interval between the second and the third nearest-neighbor interatomic distances for bcc Fe. Figure 1 shows the fitted

curve for $J_0 = 904.90177$ eV and for the original data points taken from Refs. 17 and 55. The fitted curve becomes inaccurate for small interatomic separations. We were not able to investigate this further because of the lack of *ab initio* data describing this limit. A more accurate representation for J_{ij} can be implemented once more extensive *ab initio* data and more accurate functional forms for J_{ij} become available.

For example, J_{ij} is a function of the *electronic* temperature since thermal excitations affect the Fermi-Dirac statistics of electrons and influence the equilibrium magnitudes of magnetic moments. Furthermore, in the current scheme the Heisenberg spin potential has to be interpreted as an effective interaction incorporating all the effects of the non-Heisenberg type. Since the numerical representation for J_{ij} was derived by considering systems that were only weakly noncollinear, it is unlikely that it will remain accurate for strongly noncollinear systems. A more general functional form for the spin-potential may be adopted,[56] which also includes contributions of the non-Heisenberg nature.

The equations of motion for the coordinates of atoms and the orientations of spins can be derived by using the Poisson brackets[52] or by adopting the classical equation of motion for the undamped magnetization field.[26,38] To use the Poisson brackets method, we consider the *actual* atomic spins $\mathbf{S}_k$ rather than the unit direction vectors $\mathbf{e}_i$. Starting from the atomic spin Hamiltonian,

$$H_A = -\frac{1}{2}\sum_{i,j} J_{ij}^A \mathbf{S}_i \cdot \mathbf{S}_j, \tag{6}$$

we derive the equation of motion for $\mathbf{S}_k$ as

$$\frac{d\mathbf{S}_k}{dt} = \frac{i}{\hbar}[H_A, \mathbf{S}_k] = \frac{-1}{\hbar}\left(\sum_i J_{ik}^A \mathbf{S}_i\right) \times \mathbf{S}_k. \tag{7}$$

Comparing H_A and H_{spin}, we see that Eq. (7) becomes

$$S_k \frac{d\mathbf{e}_k}{dt} = \frac{-1}{\hbar}\left(\sum_i J_{ik}\mathbf{e}_i\right) \times \mathbf{e}_k \Rightarrow \Pi_k\frac{d\mathbf{e}_k}{dt} = \mathbf{e}_k \times \left(\sum_i J_{ik}\mathbf{e}_i\right), \tag{8}$$

where $\Pi_k = \hbar S_k = \hbar M_k / g\mu_B$ and where the g factor is taken as a positive quantity. M_k is the magnitude of an atomic magnetic moment, which we evaluate directly from the DD potential.[41] Quantum-mechanical derivations of Eq. (8) are also available in the literature.[25,57,58]

B. Alternative derivation

Our equations of motion for the spin subsystem differ by a factor of Π_k from those derived by Omelyan *et al.*[45] and by Tsai *et al.*,[47,48] who also used the Poisson bracket approach. This difference is significant since the spin precession frequency depends on Π_k in a way that is analogous to how the acceleration of a particle depends on its mass. To prove the correctness of our equations, below we derive them using an alternative approach.

We start with the classical equation of motion for the undamped magnetization field,[26,38]

$$\frac{d\mathbf{M}_k}{dt} = -\gamma(\mathbf{M}_k \times \mathbf{H}_k'), \tag{9}$$

where $\gamma = g\mu_B/\hbar$ is the gyromagnetic ratio and $H_K' = -\delta H_M / \delta \mathbf{M}_k$ is the effective field. The Hamiltonian for the interacting magnetic moments is

$$H_M = -\frac{1}{2}\sum_{i,j} J_{ij}^M \mathbf{M}_i \cdot \mathbf{M}_j, \tag{10}$$

from where it follows that

$$\frac{d\mathbf{M}_k}{dt} = -\gamma\left(\mathbf{M}_k \times \sum_i J_{ik}^M \mathbf{M}_i\right). \tag{11}$$

Comparing H_M and H_{spin} and taking into account that the direction of the magnetic moment is opposite to that of the atomic spin, we transform Eq. (11) as

$$\left(\frac{M_k}{\gamma}\right)\frac{d\mathbf{e}_k}{dt} = \left(\mathbf{e}_k \times \sum_i J_{ik}\mathbf{e}_i\right), \Rightarrow \Pi_K\frac{d\mathbf{e}_k}{dt} = \left(\mathbf{e}_k \times \sum_i J_{ik}\mathbf{e}_i\right), \tag{12}$$

which is the same as Eq. (8).

Finally, the classical SLD equations of motion for the coordinates of atoms and the direction vectors of atomic spins derived from Eq. (3) are

$$\begin{cases} \dfrac{d\mathbf{R}_k}{dt} = \dfrac{\partial H}{\partial \mathbf{p}_k} = \dfrac{\mathbf{p}_k}{m_k} \\[2ex] \dfrac{d\mathbf{p}_k}{dt} = -\dfrac{\partial H}{\partial \mathbf{R}_k} = -\dfrac{\partial U}{\partial \mathbf{R}_k} + \dfrac{1}{2}\sum_{i,j}\dfrac{\partial J_{ij}}{\partial \mathbf{R}_k}(\mathbf{e}_i \cdot \mathbf{e}_j) \end{cases}, \tag{13}$$

and

$$\Pi_k\frac{d\mathbf{e}_k}{dt} = \mathbf{e}_k \times \mathbf{H}_k, \tag{14}$$

where $\mathbf{H}_k = \Sigma_i J_{ik}\mathbf{e}_i$ is the effective exchange vector field acting on spin k and $\Pi_k = \hbar S_k$ plays the part of the effective mass for the dynamics of angular motion of the atomic spin. Equations (13) and (14) show that the dynamics of the lattice and spin subsystems are explicitly coupled through the dependence of J_{ij} on atomic coordinates $\{\mathbf{R}_k\}$ via the gradient $\partial J_{ij}/\partial \mathbf{R}_k$ term in Eq. (13) and via the J_{ij} term in Eq. (14). Equations (13) and (14) do not take into account the spin-orbit coupling between the lattice and the spin subsystems.

C. Conservation of energy

To prove that the above equations of motion are consistent with the principle of energy conservation, we write,

$$\frac{dE}{dt} = \sum_k \frac{\mathbf{p}_k}{m_k}\frac{d\mathbf{p}_k}{dt} + \sum_k \frac{\partial U}{\partial \mathbf{R}_k}\frac{d\mathbf{R}_k}{dt} - \frac{1}{2}\sum_{i,j}\sum_k \frac{\partial J_{ij}}{\partial \mathbf{R}_k}\frac{d\mathbf{R}_k}{dt}(\mathbf{e}_i \cdot \mathbf{e}_j)$$
$$- \frac{1}{2}\sum_{i,j} J_{ij}\frac{d}{dt}(\mathbf{e}_i \cdot \mathbf{e}_j). \tag{15}$$

Since the last term in this equation is zero (see Appendix), we group the second and the third terms together as

$$\frac{dE}{dt} = \sum_k \frac{\mathbf{p}_k}{m_k}\frac{d\mathbf{p}_k}{dt} + \sum_k \left[\frac{\partial U}{\partial \mathbf{R}_k} - \frac{1}{2}\sum_{i,j}\frac{\partial J_{ij}}{\partial \mathbf{R}_k}(\mathbf{e}_i \cdot \mathbf{e}_j) \right]\frac{d\mathbf{R}_k}{dt}. \tag{16}$$

The expression in square brackets equals the right-hand side of the equation describing the evolution of the momentum of an atom and $d\mathbf{R}_k/dt = \mathbf{p}_k/m_k$, taken with the minus sign. We arrive at

$$\frac{dE}{dt} = \sum_k \frac{\mathbf{p}_k}{m_k}\frac{d\mathbf{p}_k}{dt} - \sum_k \frac{d\mathbf{p}_k}{dt}\frac{\mathbf{p}_k}{m_k} = 0, \tag{17}$$

that proves that the total energy is conserved if the coordinates, velocities, and the spin directions of atoms evolve according to the SLD Eqs. (13) and (14).

D. Integration algorithm

A viable numerical algorithm for integrating the spin-lattice dynamics equations must conserve energy and angular momentum in a large-scale simulation involving hundreds of thousands of atoms over a relatively long interval of time of a hundred million time steps. In our preliminary simulations, we found that the standard predictor-corrector method did not had the sufficient accuracy and could not be used in practical simulations. Omelyan et al.[44] and Tsai et al.[47,48] investigated applications of symplectic integration algorithms for both the spin and the lattice degrees of freedom. Omelyan et al.[44] also took the exchange function as a pairwise function of the interatomic distance but did not apply the method to the treatment of a realistic system. On the other hand, Tsai et al.[47,48] did not treat coupling between the lattice and the spin degrees of freedom. Both integration schemes were based on the second-order STD for the noncommuting evolution operators for the spin and the lattice degrees of freedom. In comparison with the fourth-order Runge-Kutta method, the second-order symplectic algorithm has superior accuracy.

Consider the equations of motion for a generalized set of coordinates $d\mathbf{x}/dt = L\mathbf{x}$, where L is the Liouville operator. The formal solution for the Liouville equation is $\mathbf{x}(t+\Delta t) = e^{L\Delta t}\mathbf{x}(t)$. The second-order STD formula states that if an operator is given by a sum of two terms, e.g., $C = A + B$, then,

$$e^{C\Delta t}\mathbf{x}(t) = e^{(A+B)\Delta t}\mathbf{x}(t) = e^{A(\Delta t/2)}e^{B\Delta t}e^{A(\Delta t/2)}\mathbf{x}(t) + O(\Delta t^3)$$
$$= e^{B(\Delta t/2)}e^{A\Delta t}e^{B(\Delta t/2)}\mathbf{x}(t) + O(\Delta t^3). \tag{18}$$

In the case where only the positions and velocities are treated as variables,[47,48] i.e., $L = L_r + L_v$, we write,

$$e^{L_r\tau}\{\mathbf{R}_k(t), \mathbf{p}_k(t)\} = \{\mathbf{R}_k(t+\tau), \mathbf{p}_k(t)\}$$
$$= \{\mathbf{R}_k(t) + (\mathbf{p}_k(t)/m)\tau, \mathbf{p}_k(t)\}, \tag{19}$$

and

$$e^{L_v\tau}\{\mathbf{R}_k(t), \mathbf{p}_k(t)\} = \{\mathbf{R}_k(t), \mathbf{p}_k(t+\tau)\}$$
$$= \{\mathbf{R}_k(t), \mathbf{p}_k(t) + \mathbf{F}_k(\{\mathbf{R}_k(t)\})\tau\}, \tag{20}$$

where $\mathbf{F}_k(\{\mathbf{R}_k(t)\})$ is the force evaluated at time t. The second-order velocity Verlet (VV) algorithm is equivalent to the second-order STD (Refs. 47 and 48) of the form $e^{L_v(\Delta t/2)}e^{L_r\Delta t}e^{L_v(\Delta t/2)}$.

In the spin-lattice dynamics case, the Liouville operator is given by a sum of three terms, $L = L_r + L_v + L_s$, where L_r, L_v, and L_s are the Liouville operators for the atomic coordinates, velocities, and spins, respectively. One can decompose the evolution operator in several alternative ways according to Eq. (18). Omelyan et al.[44] decomposed this evolution operator as

$$\mathbf{x}(t+\Delta t) = e^{L_v(\Delta t/2)}e^{L_r(\Delta t/2)}e^{L_s\Delta t}e^{L_r(\Delta t/2)}e^{L_v(\Delta t/2)}\mathbf{x}(t) + O(\Delta t^3), \tag{21}$$

whereas Tsai et al.[47,48] used the decomposition of the form,

$$\mathbf{x}(t+\Delta t) = e^{L_s(\Delta t/2)}e^{L_v(\Delta t/2)}e^{L_r\Delta t}e^{L_v(\Delta t/2)}e^{L_s(\Delta t/2)}\mathbf{x}(t) + O(\Delta t^3). \tag{22}$$

For convenience, we denote Omelyan's method by (v, r, s, r, v) and Tsai's decomposition by (s, v, r, v, s). In our work we use the (s, r, v, r, s) decomposition to minimize the frequency of evaluation of L_v, which is the most time consuming step of the algorithm. The three decompositions are equivalent and in each case the error is of the order of $O(\Delta t^3)$. The subrotation of each spin is performed using the method described in Ref. 44. We note that while the higher-order STDs are available in the literature,[46] the accuracy of the second-order STD-based algorithm is sufficient for simulations described in this paper.

E. Spin temperature

To perform a simulation for an open system, we need to develop a method for controlling the temperature of the spin subsystem. Note that spin orientations do not thermalize on their own in a closed microcanonical ensemble because of constraints imposed by the conservation of the total angular momentum. For example, a configuration with all the spins pointing "up" cannot exchange energy with the lattice subsystem *at any temperature of the lattice* since the conservation law, requiring that the total angular momentum stays constant, prevents any of the spins from changing its orientation. Interaction between phonons and magnons may in principle allow exchange of energy and angular momentum between the spin and the lattice subsystems in a microcanonical ensemble. However the Hamiltonian used in this paper does not contain terms such as the spin-orbit coupling that would facilitate the transfer of the angular momentum from the spin subsystem to the lattice. In this respect, the dynamics of a large closed system of interacting atomic spins is fundamentally different from the dynamics of a large closed system of interacting atoms—where collisions between the atoms eventually give rise to the statistical

equilibration of positions and velocities, asymptotically approaching those of a canonical ensemble simulation.

We introduce the notion of spin temperature by using the Langevin-type stochastic equations:[34,37]

$$\Pi_k \frac{d\mathbf{e}_k}{dt} = [\mathbf{e}_k \times (\mathbf{H}_k + \mathbf{h}_k) - \eta \mathbf{e}_k \times (\mathbf{e}_k \times \mathbf{H}_k)], \quad (23)$$

where $\mathbf{h}_k$ is a delta-correlated random fluctuation of magnetic field $\mathbf{H}_k$ satisfying the condition,

$$\langle h_i(t') h_j(t'') \rangle = \mu \delta_{ij} \delta(t' - t''). \quad (24)$$

Here μ is a parameter characterizing the amplitude of the random noise, and indices i and j refer to the Cartesian coordinates x, y, and z. In Eq. (23), η is a dimensionless damping constant, which together with the random fluctuation $\mathbf{h}_k$ describes interactions between the spin subsystem and the thermostat, and the resulting exchange of energy and angular momentum between the spin subsystem and thermodynamic reservoir. The temperature of the spin subsystem is controlled through the use of the fluctuation-dissipation theorem.[35,36] Following Brown, Jr.,[34] we identify the energy distribution for the spin subsystem, defined by a solution for the corresponding Fokker-Planck equation, with the Gibbs distribution. This gives rise to a relation between the amplitude μ of random fluctuations and the damping constant,

$$\mu = 2\Pi_k k_B T \eta, \quad (25)$$

where T is the absolute temperature of the spin thermostat. In the numerical implementation of the method, the random noise is modeled by the Gaussian random numbers.

III. APPLICATION OF THE METHOD: EXAMPLES

This section describes several applications of the method. We start with a simple case of an isolated (microcanonical ensemble) system and investigate the dynamics of adiabatic spin-lattice relaxation for a periodic array of 180° domain walls. We then generalize the treatment to the case of the Langevin random force-driven ensemble and investigate the time evolution and the equilibrium magnetic properties of homogeneous spin-polarized systems at various temperatures, where the spin-polarized atoms exchange energy and angular momentum with a thermostat.

The scalar part of the interatomic potential and the exchange function J_{ij} fully determines the dynamics of evolution of atomic coordinates and spins. Both the energy and the total angular momentum of the system remain constant during the simulation. The microcanonical simulations were performed for a system of 54 000 atoms initially placed in a regular bcc lattice with the lattice parameter $a=2.8665$ Å. The initial dimensions of the cubic simulation cell were $30 \times 30 \times 30a^3$, with periodic boundary conditions applied along x, y, and z. The spin configuration was initialized such that all the spins on the left-hand side of the simulation cell $(0 < x < 15a)$ pointed upwards, whereas the spins on the right-hand side of the cell $(15a < x < 30a)$ pointed downwards.
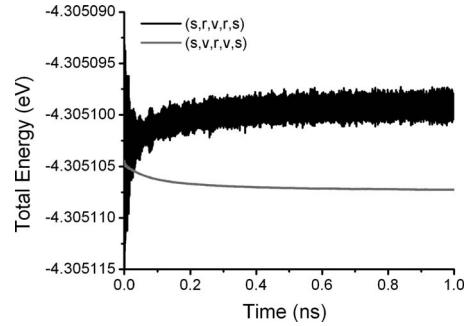
FIG. 2. The total energy per atom versus time evaluated for a microcanonical ensemble simulation of dynamical relaxation of a 180° domain wall using the (s,r,v,r,s) and (s,v,r,v,s) algorithms. The (s,r,v,r,s) algorithms is 1.6 times faster than the (s,v,r,v,s) algorithm.

Before discussing the simulations we briefly address the computational aspects of the simulation algorithm. In comparison with the conventional MD, the speed of the (s,r,v,r,s) SLD algorithm is approximately half the speed of the velocity Verlet algorithm. Furthermore, the (s,v,r,v,s) algorithm is approximately 1.6 times slower than the (s,r,v,r,s). In terms of energy conservation, Fig. 2 shows the total energy of the system as a function of time computed using the (s,r,v,r,s) and the (s,v,r,v,s) algorithms. Both algorithms perform well, and the total energy per atom remains constant within $\sim 10^{-5}$ eV, and sometimes even within $\sim 10^{-6}$ eV uncertainty bands.

A microcanonical simulation provides a convenient means for investigating the rate of transfer of energy between the lattice and the spin subsystems. In bulk bcc Fe the orbital moments of the 3d electron are nearly quenched and the coupling between the orbital moments and the lattice via the anisotropic crystal field is weak. Hence we neglect the transfer of energy between the spin and the lattice subsystems occurring via the spin-orbit interaction channel.[59] Van Kranendonk and Van Vleck[12] pointed out that spin-spin relaxation comes from the exchange interactions, which "spoil the constancy of the spatial components of magnetic moment." The spin-lattice relaxation occurs through the "modulation of the spin interaction energies, i.e., the spin waves by the crystalline vibration" or, in other words, through the variation of the exchange function due to thermal vibrations of atoms in the lattice.[24] By performing a microcanonical SLD simulation, we show how this coordinate dependence of the exchange parameter facilitates the transfer of energy between the spin and the lattice subsystems. As mentioned earlier, the energy transfer between the spin and lattice subsystems in our simulations is *not* driven by the dissipation terms in the LL and Gilbert equations. The dissipative terms in these equations drive the spin system toward gradual loss of kinetic energy and fluctuations of angular momentum, eventually resulting in a ferromagnetic collinear ground state.

In the simulations considered here, the velocities of all the atoms were initially set to zero and the energy was initially stored purely in the spatially heterogeneous spin configuration of the domain wall. Figure 3(a) shows that the process
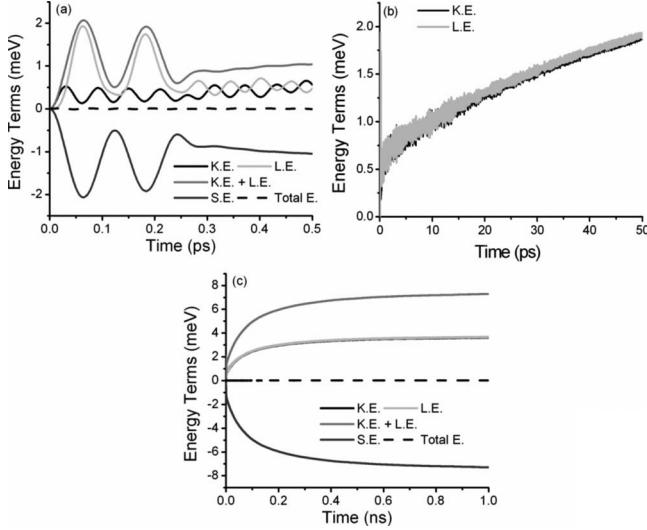
FIG. 3. Time evolution of the kinetic, the potential, and the spin energy terms determined in simulations of dynamical relaxation of a 180° domain wall and shown in the (a) 0.1 ps, (b) 10 ps, and (c) 1ns time scales. The velocities of all the atoms were initialized to zero at $t=0$. The curves show the variation of energy terms with respect to their initial values. KE and LE refer to the kinetic and the scalar (lattice) part of the potential energy defined by Eq. (3), respectively, whereas the spin energy SE refers to the last term in Eq. (3). The sum of the lattice and the spin energies equals the potential energy of the system.

FIG. 4. (Color online) The phase trajectory of an atom (left) and the spin direction (right) followed using a microcanonical ensemble simulation performed for a 54 000 atom system thermally equilibrated at $T=300$ K.

of relaxation was initiated by the spin orientation dependent forces that excited lattice vibrations at the domain boundary. These vibrations remain coherent on the time scale of approximately two periods of phonon oscillations, each occurring on the Debye time scale of ∼0.1 ps. The lattice perturbation then propagates as sound waves that collide in the center of the cell at $t \sim 0.3$ ps. The subsequent lattice relaxation illustrated in Fig. 3(b) gives rise to rapid equipartitioning of the kinetic and the potential energies *of the lattice*, occurring on the 10–20 ps time scale. This is driven primarily by the anharmonicity of the scalar part of the interatomic potential and the resulting phonon-phonon interactions. On this 10–20 ps time scale the spin subsystem remains coupled to the lattice. However, this coupling is weak in terms of its effect on the rate of intralattice energy equipartitioning. On the same 10–20 ps time scale the spin subsystem evolves into a quasiequilibrium configuration that can be approximately described as an incoherent superposition of spin waves. Figure 3(c) shows that the relaxation of the combined spin-lattice subsystem is characterized by a much longer relaxation time of the order of a nanosecond. This relaxation time now characterizes the rate of exchange of energy between the two subsystems and results in the eventual thermalization of spins and the lattice. This process is driven by the spin-phonon interaction resulting from the dependence of the exchange function on the local atomic environment. The nanosecond time scale of the spin-phonon thermalization found in our simulations agrees with the analytical estimates by Sinha and Upadhyaya.[61] The final spin-lattice thermalization occurs subject to the condition that the total angular momentum of the spin subsystem remains constant, in agreements with the total angular momentum conservation law.
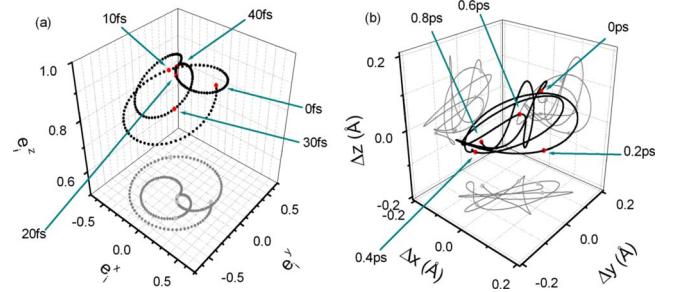
At this point, it is instructive to compare the time scales characterizing the *microscopic* evolution of the atomic and the spin degrees of freedom. Each individual atom and each individual spin are coupled to the surrounding atoms and can be treated as an open classical dynamical system evolving under variable external force. Figure 4 shows phase trajectories for the coordinates and the spin direction drawn for an arbitrarily chosen atom in a system thermalized at 300 K. We see that the characteristic time scale for the quasiperiodic motion of an atom is of the order of 0.1 ps (which is the inverse Debye frequency of the material), whereas the dynamics of precession of atomic spins is characterized by the time scale several times shorter. The fundamental difference between the three-dimensional (3D) dynamics of atoms and the two-dimensional (2D) dynamics of spins, in addition to the approximately one order of magnitude difference between the frequencies of the quasiperiodic modes of motion shown in Fig. 4, is responsible for the relatively long thermalization time scale associated with the interaction between the spin and the lattice subsystems.

Figure 5 shows that the spin configuration of the domain boundary starts relaxing at $t \approx 0.25$ ps in response to the initial rapid atomic displacements. The spin subsystem gradually loses its order, resulting in the gradual increase in the entropy of the system. At the same time, the energy of the spin system "leaks" out to the lattice subsystem. As we have already noted, this is a comparatively slow process occurring on the time scale of ∼0.25 ns. It takes about 1 ns for the full equilibrium to be established [Fig. 3(c)]. The kinetic energy of the lattice subsystem increases and the effective temperature increases from 0 K to about 28 K. By the time $t=1$ ns, the initial sharpness of the domain boundary structure vanishes. Further relaxation is prevented by the law of conservation of the angular momentum, and the final relaxed domain boundary spin configuration shown in Fig. 5 evolves into a continuously oscillating steady state.

To describe the degree of collinearity of spins in a volume containing N atoms, it is convenient to introduce the spin collinearity parameter $\xi_C = 1/N|\Sigma_i \mathbf{e}_i|$. ξ_C is a statistical measure of directional order in the spin subsystem characterizing the degree of collective orientation of spins irrespective of
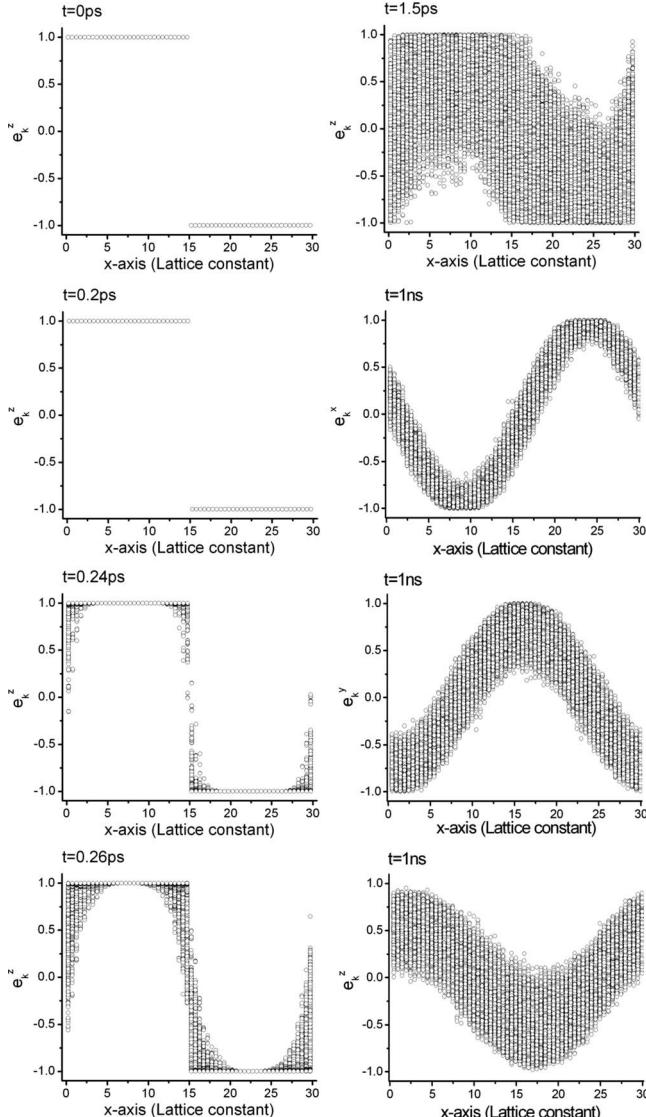
FIG. 5. Projections of atomic spins found in a microcanonical ensemble simulation of dynamical relaxation of an initially sharp magnetic domain boundary.

FIG. 6. Examples of dynamical simulations performed using the Langevin SLD algorithm for $\eta = 10^{-3}$ for several temperatures of the thermostat.

the magnitude of magnetic moments. For example, if $\xi_C = 1$ then the spin orientations are fully collinear, whereas $\xi_C = 0$ corresponds to a fully disordered spin configuration.

We now proceed from the microcanonical (NVE) to the isothermal-isobaric (NPT) simulation ensembles, and investigate a series of the Langevin type SLD simulations. Hydrostatic pressure, defined as the ensemble mean of the diagonal terms of the stress tensor, is controlled by the Berendsen method.[60] The simulation cell is allowed to expand or shrink under the stress-free condition to arrive at a steady-state configuration. The degree of collinearity of spins is characterized by the parameter ξ_C introduced above. In Fig. 6 we plot the curves showing how the spin collinearity parameter evolves for various temperatures of the thermostat. Each simulation begins with a completely aligned initial spin configuration ($\xi_C = 1$) assuming periodic boundary conditions in all three directions. The simulations were run for a sufficiently long period of time to attain equilibrium. We note that

the time variable in our simulation "does not merely label the sequential order of generated states when sampling the phase space but is related to physical time,"[37] and shows the dynamics of thermalization in the spin subsystem interacting with a thermostat. We also investigate isothermal relaxations for two different values of the damping constant $\eta = 10^{-3}$ and 10^{-4} at the thermostat temperature of 300 K. Figure 7 shows the resulting spin collinearity ξ_C as a function of time. We observe that the value of the damping constant only affects *the rate* of equilibration of the system and not the final equilibrium value of ξ_C.

Figure 8 shows the calculated equilibrium values of the spin collinearity parameter ξ_C as a function of the absolute temperature. The same graph shows the corresponding experimental data[62] and the average magnetization curve predicted by the mean-field approximation[11,13,63] in the classical limit. The experimental Curie temperature T_c of Fe is 1043 K. The calculated mean-field value of T_c obtained using the exchange function J_{ij} adopted in this paper is 1082 K. Our spin-lattice dynamics simulations predict the Curie temperature in the range between 1050 and 1100 K. Given that these results are based on the *ab initio* form for the exchange function, it is encouraging to see that the present treatment correctly describes the order/disorder nature of the ferromagnetic/paramagnetic transition in bulk bcc iron. It also lends confidence to the SLD algorithm described above. One may note that the calculations presented here are the first examples of a *dynamical* simulation of the ferromagnetic/paramagnetic phase transition performed using a method in which the emergence of spin noncollinearity at elevated temperatures results from spin-lattice coupling. The calculated spin collinearity curve is closer to the classical mean-field spin approximation than to the experimental data. This finding corroborates the conclusion of Hubbard[11] who interpreted this deviation as a result of the classical treatment of a (actual) quantum spin system.

An order/disorder ferromagnetic/paramagnetic phase transition is characterized by the disappearance of the long-range orientational order in the spin subsystem. To investigate the *short-range* orientational order in the spin subsystem remaining at temperatures exceeding the Curie temperature, we
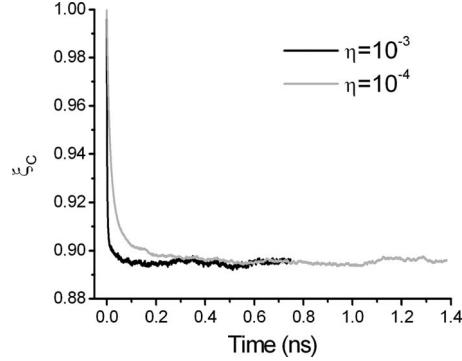
FIG. 7. Examples of Langevin SLD simulations of thermal relaxation of the spin subsystem interacting with the thermostat kept at $T=300$ K performed for two different values of the damping constant.

FIG. 8. The equilibrium magnetization curve showing the average atomic spin evaluated dynamically using the canonical ensemble simulations for various temperatures. Experimental data were taken from Ref. 62 and the mean-field approximation curve was evaluated using the method described in Ref. 63 in the classical limit.

calculate the equilibrium spatial spin-spin correlation functions (shown in Fig. 9) for the first twelve nearest-neighbor (NN) shells. It can be seen that the first and the second nearest-neighbor spins remain aligned even for temperatures significantly higher than T_c. The correlation functions remain non-negative for all the sites up to the 12th nearest neighbor.

To analyze the dynamics of atomic spins at thermal equilibrium, we evaluate the time-dependent spin-spin autocorrelation function $\langle \mathbf{e}_i(t) \cdot \mathbf{e}_i(t+\tau) \rangle = 1/N \Sigma_i \mathbf{e}_i(t) \cdot \mathbf{e}_i(t+\tau)$ obtained from an NVE simulation of a thermally equilibrated ensemble. Figure 10 shows the oscillating behavior of $\langle \mathbf{e}_i(t) \cdot \mathbf{e}_i(t+\tau) \rangle$ found for short time scales of the spin precession trajectories similar to that shown in Fig. 4, where it can be seen that the transverse component of the spin orientation vector increases due to the increase in the average precession angle treated as a function of temperature. At ~700 K the fluctuations shown in Fig. 10 reach maximum and then gradually die out. We note that in the limit $\tau \to \infty$ the autocorrelation function asymptotically approaches the square of the equilibrium spin collinearity parameter. To estimate the spin autocorrelation dephasing time, an exponential decay function was least-square fitted to the upper envelope curve for low temperatures and to the entire curve for high temperatures. The results are plotted in Fig. 11, which shows that the spin autocorrelation dephasing time is approximately equal to 10 fs. This result corroborates very well the findings of Hübner and Zhang[7] who estimated, by calculating the optical susceptibility of metallic Ni, that the dephasing time was also of the order of 10 fs.

Finally, Fig. 12 shows the difference between the equilibrium lattice constants calculated with and without taking into account the spin-lattice coupling, plotted as a function of temperature. The striking difference between the two curves shows the significant effect of spin-lattice coupling on the temperature-dependent equilibrium lattice constant, which is one of the most basic properties of the material. Experimental results[64] are also plotted for comparison. We see that taking into account spin-lattice coupling within the present scheme produces better agreement with observations even though deviations from experimental values still exist. We
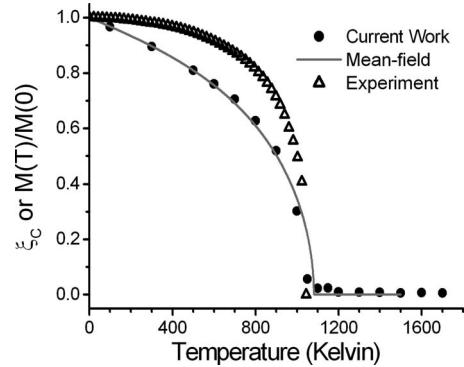
note the inflection point of the predicted curve near the Curie temperature. This is evidently related to the spin part of the Hamiltonian and to the effect of spin-spin correlations on the interatomic forces. Indeed, interatomic interactions at 0 K can be approximated by functions that depend only on the atomic configuration. At a finite temperature the collective behavior of spins becomes important. The phase stability of the lattice is maintained by the combined action of the two fluctuating forces, one arising from the scalar interatomic potential and the other from the gradient of the exchange function in the Heisenberg spin-spin Hamiltonian. The temperature dependence of the first contribution comes from the anharmonicity of scalar interatomic forces, whereas the second part comes from the effect of spin fluctuations (magnons). Comparing the values of the lattice constant calculated with and without the spin-lattice interaction, we conclude that the effect of the exchange interaction at a finite temperature favors thermal expansion of the lattice. A natural line for the future development of spin-lattice dynamics simulations will include an investigation into a suitable functional form and into better definition of parameters for the effective classical Hamiltonians of interacting spin-lattice systems.
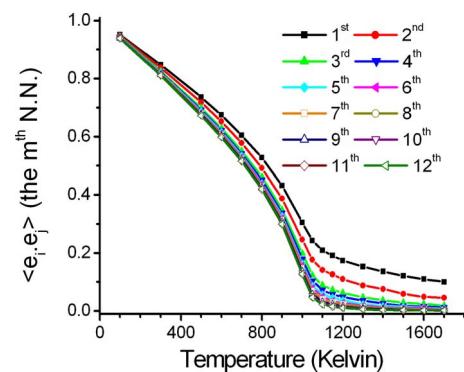
FIG. 9. (Color online) The spin-spin spatial correlation functions shown as functions of absolute temperature for the first, second, …, 12th nearest-neighbor atoms.
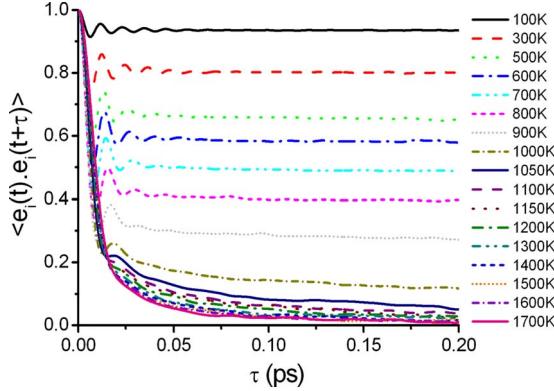
FIG. 10. (Color online) The time-dependent spin-spin on-site autocorrelation functions evaluated dynamically using the microcanonical ensemble simulations performed for fully thermalized initial configurations.

IV. SUMMARY AND CONCLUSIONS

Large-scale molecular dynamics simulations of magnetic materials, such as ferromagnetic iron or iron-based magnetic alloys, so far have neglected coupling between the spins (or magnetic moments) and the lattice degrees of freedom of atoms. This restricts the applicability of simulations to very low temperatures or to systems where the spin-lattice coupling is negligible. A thermodynamically accurate simulation of a ferromagnetic material at a reasonably high (e.g., room) temperature requires treating the flow of energy between the lattice and the spin subsystems. It also requires that the coupling between the spin and lattice dynamics be explicitly considered as a part of the overall dynamics of the system. In the present paper, the spin-lattice dynamics (SLD) equations of motion are derived from a classical Hamiltonian expressed in terms of the magnetic interatomic potential[40,41] and the Heisenberg spin-spin interaction with a pair-wise exchange function. The equations of motion are integrated using the second-order Suzuki-Trotter decomposition for the noncommuting operators of evolution for coordinates and spins, and the spin temperature is introduced via the fluctuation-dissipation theorem. The scheme is first validated for energy conservation in a simulation of adiabatic relaxation of a periodic array of 180° domain walls at 0 K in ferromagnetic bcc iron. The relaxation is found to increase the temperature of the lattice from 0 to 28 K. Then, we investigated the dynamics of thermalization under the NPT conditions where the system exchanges energy and angular momentum with an external thermal reservoir. The temperature dependence of the average magnetization found in simulations agrees with experimental observations within the limits imposed by the classical statistical mechanics. We also found that the dynamics of the spin degrees of freedom affects the observed equilibrium properties of the system, for example, the coefficient of thermal expansion. Comparison with experiments and with the case where atomic spin dynamics was neglected illustrates the significance of including the spin-orientation degrees of freedom in dynamical simulations of magnetic materials.
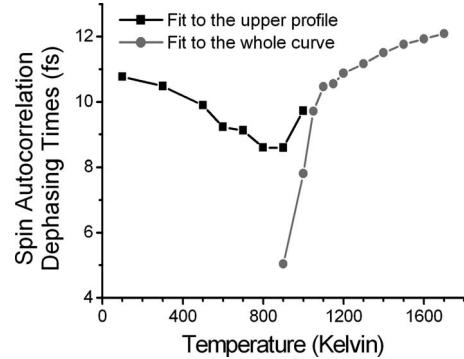
FIG. 11. The spin autocorrelation dephasing times for the curves shown in Fig. 10.

The SLD algorithm exhibits good stability as a simulation method and the predicted behavior agrees well with what is expected physically and with experiments where the relevant data are available. The numerical implementation is accurate and suitable for simulating systems containing many ($\sim 10^6$) atoms over relatively long intervals of time (> 1 ns). The computational resources required for the implementation of the algorithm are only twice those needed for a conventional MD simulation. In this regard, the present scheme is capable of simulating systems that are well beyond the reach of any electronic structure-based spin-lattice dynamics approach.
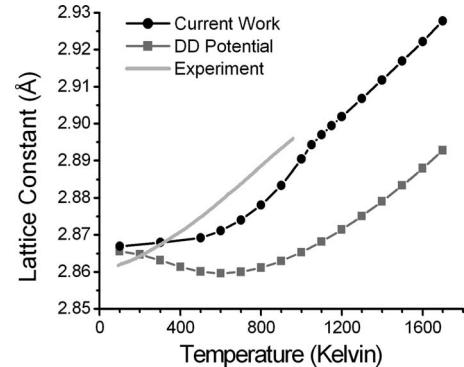
FIG. 12. Equilibrium zero pressure lattice constant of bcc iron evaluated using SLD simulations and conventional MD simulations performed using the magnetic DD potential. Experimental data taken from Ref. 64 are also shown for comparison.

APPENDIX

The proof of the relation $\Sigma_{i,j}J_{ij}d/dt(\mathbf{e}_i\cdot\mathbf{e}_j)=0$.

$$\sum_{i,j}J_{ij}\frac{d}{dt}(\mathbf{e}_i\cdot\mathbf{e}_j)=\sum_{i,j}J_{ij}\left[\mathbf{e}_i\cdot\frac{d\mathbf{e}_j}{dt}+\frac{d\mathbf{e}_i}{dt}\cdot\mathbf{e}_j\right]$$

$$=\sum_{i,j}J_{ij}\left[\mathbf{e}_i\cdot\frac{1}{\Pi_j}\mathbf{e}_j\times\mathbf{H}_j+\frac{1}{\Pi_i}\mathbf{e}_i\times\mathbf{H}_i\cdot\mathbf{e}_j\right].$$

(A1)

Since the exchange function is symmetric, i.e., $J_{ij}=J_{ji}$,

$$\sum_{i,j}J_{ij}\frac{d}{dt}(\mathbf{e}_i\cdot\mathbf{e}_j)=\sum_{i,j}\frac{2}{\Pi_j}J_{ij}[\mathbf{e}_i\cdot\mathbf{e}_j\times\mathbf{H}_j]$$

$$=\sum_{i,j}\frac{2}{\Pi_j}J_{ij}\left[\mathbf{e}_i\cdot\mathbf{e}_j\times\sum_k J_{kj}\mathbf{e}_k\right]$$

$$=\sum_j\frac{2}{\Pi_j}\left[\left(\sum_i J_{ij}\mathbf{e}_i\right)\cdot\mathbf{e}_j\times\left(\sum_k J_{kj}\mathbf{e}_k\right)\right].$$

(A2)

Since $\Sigma_i J_{ij}\mathbf{e}_i=\Sigma_k J_{kj}\mathbf{e}_k$ and for any arbitrary two vectors $\mathbf{A}\cdot[\mathbf{B}\times\mathbf{A}]=0$, we find that $\Sigma_{i,j}J_{ij}d/dt(\mathbf{e}_i\cdot\mathbf{e}_j)=0$.

---

*Corresponding author. chung.woo@polyu.edu.hk

[1] S. A. Wolf, D. D. Awschalom, R. A. Buhrman, J. M. Daughton, S. von Molnár, M. L. Roukes, A. Y. Chtchelkanova, and D. M. Treger, Science **294**, 1488 (2001).

[2] A. R. Rocha, V. M. García-Suárez, S. W. Bailey, C. J. Lambert, J. Ferrer, and S. Sanvito, Nat. Mater. **4**, 335 (2005).

[3] C. Chappert, A. Fert, and C. Nguyen van Dau, Nat. Mater. **6**, 813 (2007).

[4] C. Stamm, I. Tudosa, H. C. Siegmann, J. Stöhr, A. Y. Dobin, G. Woltersdorf, B. Heinrich, and A. Vaterlaus, Phys. Rev. Lett. **94**, 197603 (2005).

[5] W. K. Hiebert, G. E. Ballentine, and M. R. Freeman, Phys. Rev. B **65**, 140404(R) (2002).

[6] W. Hübner and K. H. Bennemann, Phys. Rev. B **53**, 3422 (1996).

[7] W. Hübner and G. P. Zhang, Phys. Rev. B **58**, R5920 (1998).

[8] G. P. Zhang and W. Hübner, Phys. Rev. Lett. **85**, 3025 (2000).

[9] J. H. Van Vleck, Phys. Rev. **57**, 426 (1940).

[10] J. Hubbard, Proc. R. Soc. London, Ser. A **276**, 238 (1963).

[11] J. Hubbard, Phys. Rev. B **19**, 2626 (1979); J. Hubbard, *ibid.* **20**, 4584 (1979).

[12] J. Van Kranendonk and J. H. Van Vleck, Rev. Mod. Phys. **30**, 1 (1958).

[13] J. H. Van Vleck, Rev. Mod. Phys. **17**, 27 (1945).

[14] B. E. Argyle, S. H. Charap, and E. W. Pugh, Phys. Rev. **132**, 2051 (1963).

[15] O. Grotheer, C. Ederer, and M. Fähnle, Phys. Rev. B **62**, 5601 (2000).

[16] Ph. Kurz, F. Förster, L. Nordström, G. Bihlmayer, and S. Blügel, Phys. Rev. B **69**, 024415 (2004).

[17] S. Morán, C. Ederer, and M. Fähnle, Phys. Rev. B **67**, 012407 (2003).

[18] O. Grotheer, C. Ederer, and M. Fähnle, Phys. Rev. B **63**, 100401(R) (2001).

[19] S. Y. Savrasov, Phys. Rev. Lett. **81**, 2570 (1998).

[20] Y. Kakehashi, S. Akbar, and N. Kimura, Phys. Rev. B **57**, 8354 (1998).

[21] Y. Kakehashi, Philos. Mag. **86**, 2603 (2006).

[22] Y. Kakehashi, Adv. Phys. **53**, 497 (2004).

[23] Y. Kakehashi and J. H. Samson, Phys. Rev. B **33**, 298 (1986).

[24] C. Kittel and E. Abrahams, Rev. Mod. Phys. **25**, 233 (1953).

[25] V. P. Antropov, M. I. Katsnelson, M. van Schilfgaarde, and B. N. Harmon, Phys. Rev. Lett. **75**, 729 (1995); V. P. Antropov, M. I. Katsnelson, B. N. Harmon, M. van Schilfgaarde, and D. Kusnezov, Phys. Rev. B **54**, 1019 (1996).

[26] T. L. Gilbert, IEEE Trans. Magn. **40**, 3443 (2004).

[27] S. M. Bhagat, J. R. Anderson, and L. L. Hirst, Phys. Rev. Lett. **16**, 1099 (1966); S. M. Bhagat, J. R. Anderson, and Ning Wu, Phys. Rev. **155**, 510 (1967).

[28] S. M. Bhagat and P. Lubitz, Phys. Rev. B **10**, 179 (1974).

[29] J. F. Cochran, J. M. Rudd, W. B. Muir, G. Trayling, and B. Heinrich, J. Appl. Phys. **70**, 6545 (1991).

[30] F. Schreiber, J. Pflaum, Z. Frait, Th. Mühge, and J. Pelzl, Solid State Commun. **93**, 965 (1995).

[31] C. Scheck, L. Cheng, I. Barsukov, Z. Frait, and W. E. Bailey, Phys. Rev. Lett. **98**, 117601 (2007).

[32] R. Urban, G. Woltersdorf, and B. Heinrich, Phys. Rev. Lett. **87**, 217204 (2001).

[33] D. Steiauf and M. Fähnle, Phys. Rev. B **72**, 064450 (2005).

[34] W. F. Brown, Jr., Phys. Rev. **130**, 1677 (1963).

[35] S. Chandrasekhar, Rev. Mod. Phys. **15**, 1 (1943).

[36] R. Kubo, Rep. Prog. Phys. **29**, 255 (1966).

[37] J. L. García-Palacios and F. J. Lázaro, Phys. Rev. B **58**, 14937 (1998).

[38] M. Fähnle, R. Drautz, R. Singer, D. Steiauf, and D. V. Berkov, Comput. Mater. Sci. **32**, 118 (2005).

[39] K. Kadau, M. Gruner, P. Entel, and M. Kreth, Phase Transitions **76**, 355 (2003).

[40] S. L. Dudarev and P. M. Derlet, J. Phys.: Condens. Matter **17**, 7097 (2005); **19**, 239001 (2007).

[41] P. M. Derlet and S. L. Dudarev, Prog. Mater. Sci. **52**, 299 (2007).

[42] G. J. Ackland, J. Nucl. Mater. **351**, 20 (2006).

[43] P. W. Ma, W. C. Liu, C. H. Woo, and S. L. Dudarev, J. Appl. Phys. **101**, 073908 (2007).

[44] I. P. Omelyan, I. M. Mryglod, and R. Folk, Phys. Rev. Lett. **86**, 898 (2001).

[45] I. P. Omelyan, I. M. Mryglod, and R. Folk, Phys. Rev. E **64**, 016105 (2001).

[46] I. P. Omelyan, I. M. Mryglod, and R. Folk, Phys. Rev. E **66**, 026701 (2002).

[47] S. H. Tsai, M. Krech, and D. P. Landau, Braz. J. Phys. **34**, 382 (2004).

[48] S. H. Tsai, H. K. Lee, and D. P. Landau, Am. J. Phys. **73**, 615

(2005).

[49] S. L. Dudarev and P. M. Derlet, J. Comput.-Aided Mater. Des. **14**, Suppl. 1, 129 (2007).

[50] A. V. Ruban, S. Khmelevskyi, P. Mohn, and B. Johansson, Phys. Rev. B **75**, 054402 (2007).

[51] S. Shallcross, A. E. Kissavos, V. Meded, and A. V. Ruban, Phys. Rev. B **72**, 104437 (2005).

[52] L. A. Turski, Phys. Rev. A **30**, 2779 (1984).

[53] T. Holstein and H. Primakoff, Phys. Rev. **58**, 1098 (1940).

[54] A. J. Dekker, *Solid State Physics* (Prentice-Hall, Englewood Cliffs, NJ, 1957).

[55] R. F. Sabiryanov and S. S. Jaswal, Phys. Rev. Lett. **83**, 2062 (1999).

[56] R. Drautz and M. Fähnle, Phys. Rev. B **72**, 212405 (2005); **69**, 104404 (2004).

[57] S. V. Halilov, H. Eschrig, A. Y. Perlov, and P. M. Oppeneer, Phys. Rev. B **58**, 293 (1998).

[58] M. Fähnle and D. Steiauf, in *Handbook of Magnetism and Advances Magnetic Materials I*, edited by H. Kronmuller and S. Parkin (Wiley, New York, 2007).

[59] J. Kuneš and V. Kamberský, Phys. Rev. B **65**, 212411 (2002).

[60] M. P. Allen and D. J. Tildesley, *Computer Simulation of Liquids* (Oxford University Press, New York, 1987).

[61] K. P. Sinha and U. N. Upadhyaya, Phys. Rev. **127**, 432 (1962).

[62] J. Crangle and G. M. Goodman, Proc. R. Soc. London, Ser. A **321**, 477 (1971).

[63] U. Rössler, *Solid State Theory* (Springer, New York, 2004), pp. 175–179.

[64] F. C. Nix and D. MacNair, Phys. Rev. **60**, 597 (1941).